universe

MDPI

Article

The Upcoming GAMMA-400 Experiment

Sergey I. Suchkov [1,*], Irina V. Arkhangelskaja [2], Andrey I. Arkhangelskiy [2], Aleksey V. Bakaldin [3], Irina V. Chernysheva [2], Arkady M. Galper [1,2], Oleg D. Dalkarov [2], Andrey E. Egorov [1], Maxim D. Kheymits [2], Mikhail G. Korotkov [2], Aleksey A. Leonov [1,2], Svetlana A. Leonova [4], Alexandr G. Malinin [2], Vladimir V. Mikhailov [2], Pavel Yu Minaev [1,5], Nikolay Yu. Pappe [1], Mikhail V. Razumeyko [1], Nikolay P. Topchiev [1] and Yuri T. Yurkin [2]

1 Lebedev Physical Institute of the Russian Academy of Sciences, Moscow 119991, Russia
2 Moscow Engineering Physics Institute, National Research Nuclear University "MEPhI", Moscow 115409, Russia
3 Scientific Research Institute for System Analysis of the Russian Academy of Sciences, Moscow 117218, Russia
4 The Department of General Subjects, Dubna State University, Branch "Protvino", Moscow Region, Protvino 142281, Russia
5 Space Research Institute, Moscow 117997, Russia
* Correspondence: soutch@mail.ru

Abstract: The upcoming GAMMA-400 experiment will be implemented aboard the Russian astrophysical space observatory, which will be operating in a highly elliptical orbit over a period of 7 years to provide new data on gamma-ray emissions and cosmic-ray electron + positron fluxes, mainly from the galactic plane, the Galactic Center, and the Sun. The main observation mode will be a continuous point-source mode, with a duration of up to ~100 days. The GAMMA-400 gamma-ray telescope will study high-energy gamma-ray emissions of up to several TeV and cosmic-ray electrons + positrons up to 20 TeV. The GAMMA-400 telescope will have a high angular resolution, high energy and time resolutions, and a very good separation efficiency for separating gamma rays from the cosmic-ray background and the electrons + positrons from protons. A distinctive feature of the GAMMA-400 gamma-ray telescope is its wonderful angular resolution for energies of >30 GeV (0.01° for E_γ = 100 GeV), which exceeds the resolutions of space-based and ground-based gamma-ray telescopes by a factor of 5–10. GAMMA-400 studies can reveal gamma-ray emissions from dark matter particles' annihilation or decay, identify many unassociated, discrete sources, explore the extended sources' structures, and improve the cosmic-ray electron + positron spectra data for energies of >30 GeV.

Keywords: gamma-ray emission; gamma-ray telescope; gamma-ray bursts; dark matter particles; cosmic-ray electron + positron fluxes

Citation: Suchkov, S.I.; Arkhangelskaja, I.V.; Arkhangelskiy, A.I.; Bakaldin, A.V.; Chernysheva, I.V.; Galper, A.M.; Dalkarov, O.D.; Egorov, A.E.; Kheymits, M.D.; Korotkov, M.G.; et al. The Upcoming GAMMA-400 Experiment. *Universe* **2023**, *9*, 369. https://doi.org/10.3390/universe9080369

Academic Editors: Alexandre Marcowith and Vera Georgievna Sinitsyna

Received: 7 June 2023
Revised: 14 July 2023
Accepted: 25 July 2023
Published: 14 August 2023

1. Introduction

A significant contribution to astrophysical research has been made with gamma-ray astronomy in recent decades. Since 2008, the Fermi-LAT gamma-ray telescope has been continually used to observe high-energy gamma-ray emissions in space. The fourth Fermi-LAT catalog [1] contains 6658 sources, including various classes of objects in the energy range of 50 MeV to 1000 GeV. In spite of great progress, many problems have not yet been solved; ~30% of gamma-ray sources in the fourth catalog are still unidentified. Fermi-LAT operates in scanning mode, and the source observation time is only ~15% of the operation time [2]. The ground-based facilities H.E.S.S., MAGIC, VERITAS, and others have observed emissions from only ~250 gamma-ray sources in the energy range of above ~100 GeV (http://tevcat.uchicago.edu/, accessed on 2 August 2023). In order to identify many unassociated gamma-ray sources, it is necessary to perform long-term, continuous observations with better angular and energy resolutions than the existing telescopes.

The high-energy gamma sky consists of Milky Way galactic sources like pulsars and SNRs and extragalactic sources, mainly galactic gamma rays, which constitute roughly half of the identified emitters at energies of more than E > 100 MeV [1]. Most of the weak γ-ray emissions of numerous galactic cosmic rays powered by stellar explosions are produced in the nuclear collisions of pions or in pulsars and pulsar wind nebulae. Fermi_LAT was able to detect Andromeda (M31) using HE (high-energy) rays. It is still not clear whether M31 is an extended source or composed of two point sources, as proposed in [3]. The possible presence of dark matter in M31 could lead to the production of an additional gamma-ray flux. Because of the specifics of the Andromeda galaxy's disk orientation (slightly inclined to the line of sight), the difference in energies could arise from photons from the two hemispheres of Andromeda's halo. It was reported in [4] that such an asymmetry could be at the level of several tens of percents. The better spatial resolution of Fermi_LAT's successor would be useful in achieving a clear understanding of the origin of M31's emission.

Active galactic nuclei (AGNs) are black holes which are powered by infalling gas. AGNs are the most powerful astrophysical sources, with known luminosities of up to 10^{41} W. Radio-loud AGNs with jets represent the majority of known extragalactic gamma-ray sources in the Fermi_LAT catalog [1]. As reported in [5], the combination of radio-band antennas, optical telescopes, X-ray telescopes, Fermi_LAT, and the current generation of ground Cherenkov telescopes, provide the opportunity to characterize the spectral energy distributions of blazars of over 15 or more decades in energy. The most remarked-upon feature of this distribution is its two-hump shape, with the second peak in the ~10 MeV region. But the Fermi_LAT tracker is sensitive enough above ~100 MeV that the lack of spectral observations in the ~1–100 MeV range has surely hampered blazar studies [5].

Searching for and studying gamma-ray bursts (GRBs) are of great interest [6–8]. High-level GRB statistics in the sub-Mev range with more than 13,000 bursts are provided at http://www.ssl.berkeley.edu/ipn3/masterli.html (accessed on 2 August 2023). In this energy range, "classical", highly variable prompt emission is seen as a superposition of short, FRED (fast rise and exponential decay)-like pulses. The sub-MeV emission is usually associated with the internal shocks of a GRB's central engine, but a detailed physical model has not been developed yet. High-energy (above 100 MeV) emissions of GRBs were detected in a couple hundred bursts in Fermi-LAT and CGRO/EGRET experiments [6]. Recently, sub-TeV emission was also been detected in a few bursts in the HESS and MAGIC experiments. Neither the nature of the high-energy component nor whether the maximum photon energy could be generated by a GRB central engine is clear. This high-energy component could be connected with an afterglow—the propagation of a relativistic jet (external shocks). This is confirmed by the temporal behavior of the high-energy component and its spectral shape for several bursts (e.g., GRB 130427A and GRB 190114C). However, in some cases, the temporal and spectral characteristics of the high-energy emission point to its connection with a sub-MeV emission. Therefore, there is at least bimodal behavior demonstrated by the high-energy emission: a separate emission mechanism vs. the extension of the low-energy emission to high energies. Observations with high signal-to-noise ratios are important in the intermediate energy range of (10, 100) MeV to investigate the connection of regular, sub-MeV emissions to high-energy emissions. GAMMA-400 shows a higher level of sensitivity in this range (in simulations) and could shed light on the problem.

The next problem is to study dark matter (DM) particles via indirect gamma-ray detection. Indirect detection consists of recording th annihilation or decay of gamma-ray products. Weakly interacting massive particles (WIMPs) with masses between several GeV and several TeV are still considered to be the most probable candidates (e.g., [9]) responsible for DM. WIMPs can annihilate or decay with gamma-ray production. They can produce both excess in a continuous energy spectrum and narrow gamma-ray lines. Axion-like particles (ALPs) are also proposed as candidate particles for DM (e.g., [10]). Searching for and studying the emission of gamma rays from DM particles with better angular and energy resolutions remain some of the central goals.

The high-precision measurement of CR electron + positron fluxes of energies up to ~4.8-TeV is an important problem in the light of data obtained from many experiments such as ATIC [11], Fermi-LAT [12], PAMELA [13], AMS-2 [14], CALET [15], DAMPE [16], MAGIC [17], VERITAS [18], and H.E.S.S. [19]. These experiments have revealed several features of the spectral shapes of their fluxes, and they sometimes do not agree. It is necessary to improve the electron + positron flux data for energies up to 20 TeV.

Therefore, new space-based experiments to study gamma-ray emissions in the energy range of up to several TeV, as well as CR electron + positron fluxes of up to several tens of TeV, with better angular and energy resolutions are required.

2. The GAMMA-400 Gamma-Ray Telescope

The GAMMA-400 (Gamma Astronomical Multifunctional Modular Apparatus) gamma-ray telescope, with an initial upper energy limit of 400 GeV, was first proposed in 1988 [20] and has been developed further since then [21–23]. Its current physical scheme is shown in Figure 1.

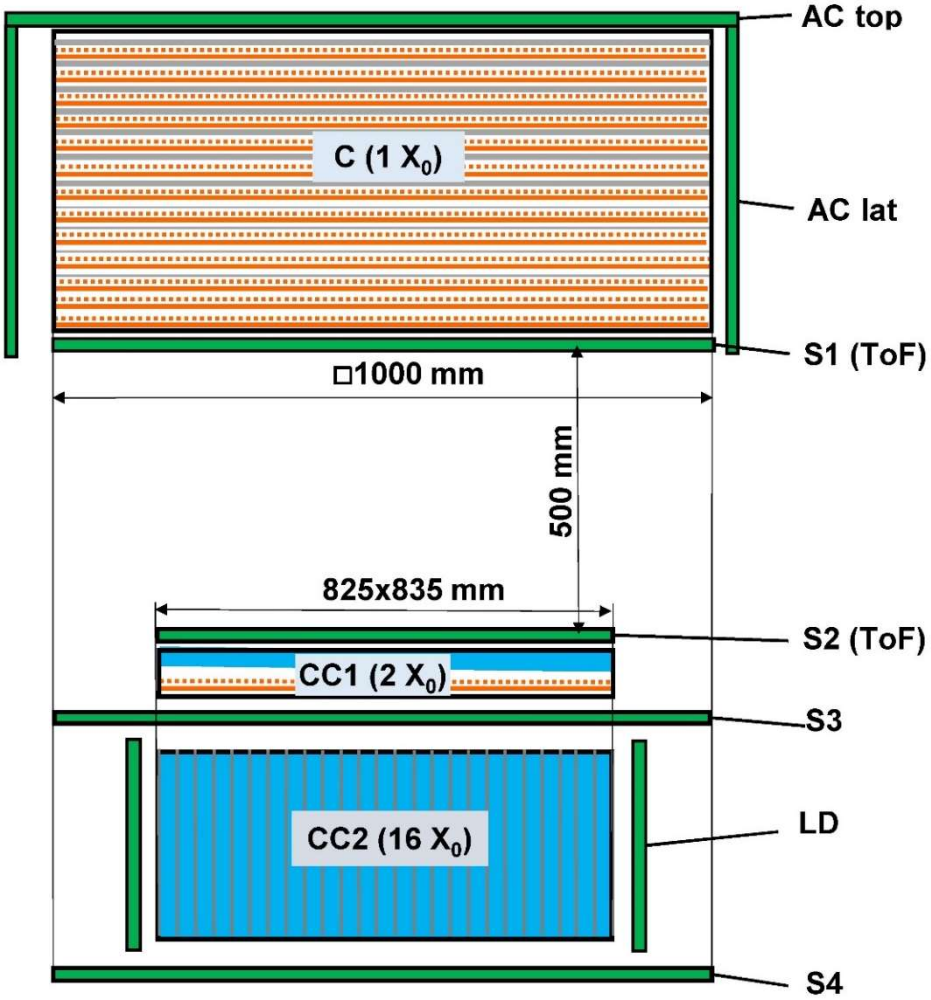

Figure 1. The GAMMA-400 gamma-ray telescope's physical scheme: an anticoincidence system, AC top, and four AC lat detectors, a converter–tracker, C, a time-of-flight system, ToF, from the S1 and S2 detectors, a two-part calorimeter, CC1 and CC2, lateral detectors, LDs, a detector, S3, and a shower leakage detector, S4.

The GAMMA-400 gamma-ray telescope consists of the following:

- A scintillation anticoincidence system, AC top, and four lateral AC detectors, AC lat. All anticoincidence detectors are made of two layers of scintillation plastic strips. The

anticoincidence system has an efficiency of ~0.9999 for detecting incoming charged particles and a time resolution of ~200 ps;

- The converter–tracker, C (~1 X_0, X_0 is the radiation interaction length), made from scintillating fibers (SciFi). The converter–tracker consists of 13 detector plane pairs made of SciFi assemblies. The top seven pairs of planes have tungsten (W) converter foils of 0.1 X_0. The next four pairs of planes contain tungsten converter foils that are 0.025 X_0 thick in each plane. The bottom two pairs of planes have no tungsten;
- Time-of-flight system, ToF, comprising the scintillation detectors S1 and S2 (the ToF signal means that the time of the S1 response must be earlier than the time of the S2 response). A distance of 500 mm between these detectors provides a sufficient flight base for the effective rejection of particles coming from the lower hemisphere with a separation coefficient of ~1000. The ToF time resolution is ~200 ps;
- A two-part electromagnetic calorimeter, comprising CC1 (2 X_0) and CC2 (~16 X_0). The pre-shower CC1 contains two blocks of CsI(Tl) scintillation crystals and the SciFi detector plane. CC2 consists of CsI(Tl) crystal columns. The total thickness of the CC1 and CC2 calorimeter is ~18 X_0 (~0.9 λ_0) and ~43 X_0 (~2.0 λ_0) for vertical and lateral particle detection, respectively (λ_0 is the hadronic interaction length);
- Four lateral scintillation detectors, LDs, located around the CC2 calorimeter for detecting particles from lateral directions;
- Scintillation detectors, S3, and shower leakage, S4. These detectors are necessary for improving hadronic and electromagnetic shower separation.

The electronic units include the system of trigger formation (ST), the scientific data acquisition system (SDAS), and other electronic units. Two-star sensors with an accuracy greater than 3″ and thermal control systems are also presented.

Incident gamma rays pass without interaction with AC and are converted into electron–positron pairs in C. The electron–positron pairs pass through the C and ToF and produce an electromagnetic shower in CC1, S3, CC2, and S4. In all the layers of the C, S1, S2, CC1, S3, CC2, S4, and LD, the energy deposits are measured.

The direction of the incidence particles is determined by reconstructing the conversion point and the electromagnetic shower axis using the SciFi coordinate detectors in the C and CC1.

High-energy (E_γ > 5 GeV) gamma rays interact with the GAMMA-400 gamma-ray telescope's detector matter and create a backscattering of secondary particles (mainly 1-MeV photons). These secondary particles can interact in the AC and produce a veto signal, excluding the primary gamma rays. To exclude this effect, all scintillation detectors are constructed as two-layer segmented strips, additional trigger logic for detecting high-energy particles is organized, and time analyses of signals in the AC, S1 (ToF), S2 (ToF), and S3 detectors are conducted.

The GAMMA-400 gamma-ray telescope's energy range is from ~20 MeV to several TeV and from ~1 GeV to several tens of TeV for gamma rays and CR electrons + positrons, respectively. The maximum field of view (FoV) for incident particles from the top-down direction is ±45°. The energy of low-energy gamma rays in the C, S1 and S2 is measured after the conversion of gamma rays in the last six planes (Figure 1, four planes with 0.025 X_0-tungsten and two without tungsten).

In contrast to previous calculations [23], in this study, a trigger based on the scintillation detector response times was used due to the very good time resolutions of the detectors. The basic characteristics were re-calculated, but they remained practically the same, confirming the correctness of the new method.

The main trigger of the GAMMA-400 telescope (with no signal in the AC and with the presence of a ToF signal) is as follows:

$$\overline{AC_{SP1}} \times ToF, \quad (1)$$

where

$$\overline{\mathrm{AC_{SP1}}} = \overline{\mathrm{AC(thesamepositionstrip)}}\Big|[\mathrm{timeAC} > \mathrm{timeS1}]; \quad (2)$$

$$\begin{aligned}&\mathrm{AC(the\ same\ position\ strip)}\\&= \mathrm{AC_{TOP}(the\ same\ position\ strip)}|\mathrm{AC_{LAT}(the\ same\ position\ strip)}\end{aligned} \quad (3)$$

means that in both layers of any AC detector, the strips located one above the other have a signal [timeAC > timeS1], meaning that the AC response time is later than the S1 response time, ToF = S1 × S2 × [timeS1 < timeS2].

The $\mathrm{AC_{SP1}}$ logic construction takes into account the possible influence of backscattering particles (which are mainly generated in calorimeter CC2). These backscattering particles have an energy distribution peak of ~1 MeV. Analyzing each layer of the AC detectors separately and taking into account that the electronic threshold in each 1 cm thick plastic scintillator strip is ~0.5 MeV, it is possible to retain useful events against backscattering particles. For this purpose, the relative location of the impacted scintillation plastic strip in the neighboring layers of each AC detector is checked. Then, only the events involving a scintillation plastic strip hit in each layer in the same position (one directly against another) are marked by veto. Other events accompanied by backscattering particles in the AC detectors not having hit the scintillation plastic strip in each layer in the same position are retained for subsequent analysis.

2.1. Gamma-Ray Detection

Gamma-400 simulations were performed using GEANT4. An example of a 100 GeV gamma-ray energy release simulation in the gamma-ray telescope's detectors is shown in Figure 2. The gamma-ray telescope's detectors are shown in color if the response exists. In this figure, the GAMMA-400 telescope's two projection responses are shown on the left and on the right of Figure 2. In the center, the CC2 view from above is demonstrated together with the AC lat detector. It is shown that a vertical gamma-ray quantum is converted into an electron–positron pair in the upper converter layer, the track goes through the whole converter, the hits are presented in S1, S2, S3, and S4, and the shower in CC1 and the shower in CC2 begin.

Some calculations were performed in which it was necessary to analyze the time consequence of the signals produced in S1(ToF) and S2(ToF), taking into account the time resolution obtained from the test beam calibration and the ability to reconstruct the particle's track and restore the particle's energy. As a result, some dependences are presented as follows:

(1) The on-axis effective area, depending on the energy (Figure 3) using triggers, is as follows:

$$\overline{\mathrm{AC}} \times \mathrm{ToF\ (black)}, \quad (4)$$

$$\overline{\mathrm{AC_{SP}}} = \overline{\mathrm{AC(the\ same\ position\ strip)}}\ \mathrm{(red)}, \quad (5)$$

$$\overline{\mathrm{AC_{SP1}}} = \overline{\mathrm{AC(the\ same\ position\ strip)}}\Big|[\mathrm{timeAC_{SP1}} > \mathrm{timeS1}]\ \mathrm{(green)}, \quad (6)$$

$$\overline{\mathrm{AC_{SP2}}} = \overline{\mathrm{AC(the\ same\ position\ strip)}}\Big|[\mathrm{timeAC_{SP1}} > \mathrm{timeS2}]\ \mathrm{(blue)}. \quad (7)$$

As can be seen from Figure 3, when using only the trigger $(\overline{\mathrm{AC}} \times \mathrm{ToF})$, the effective area begins to decrease at an energy of more than 10 GeV due to backscattering particles. Using the triggers with $\overline{\mathrm{AC_{SP1}}}$ or $\overline{\mathrm{AC_{SP2}}}$ provides an effective area of ~4000 $\mathrm{cm^2}$ and up to several TeV. If an additional analysis is used, providing the possibility to reconstruct the particle's track and to restore its energy, the effective area estimation ($\mathrm{S_{eff}}$) provides ~3200 $\mathrm{cm^2}$.

(2) The GAMMA-400 telescope's angular resolution, depending on energy, in comparison with Fermi-LAT and CTA (https://www.cta-observatory.org/science/ctao-performance/#1472563157648-91558872-faf1, accessed on 2 August 2023) (Figure 4). The angular resolution for E_γ = 100 GeV is ~0.01°. The improvement in angular resolution was achieved via analog readout in the coordinate detectors, in addition to the long arm between the coordinate detectors in the C and CC1.

(3) The on-axis energy resolution, depending on the energy, in comparison with Fermi-LAT and CTA (https://www.cta-observatory.org/science/ctao-performance/#1472563318157-d0191bc5-0280, accessed on 2 August 2023) (Figure 5). The energy resolution for E_γ = 100 GeV is ~2%.

The CC2 prototype was manufactured and calibrated on a positron beam using an S-25R electron synchrotron (Lebedev Physical Institute, Troitsk), and an energy resolution of ~10% at an energy of 300 MeV was obtained [22].

The separation of gamma rays from the background of charged particles and gamma rays emerging from the GAMMA-400 aperture plays an important role. The AC and ToF prototypes were manufactured and calibrated on a positron beam on an S-25R electron synchrotron in the energy range of 100-300 MeV. A high efficiency of charged particle detection equal to ~0.9999 for the AC system and a high coefficient of event separation coming from the top-down and down-top directions of ~1000 for the ToF system were obtained. Taking into account the separation of the electromagnetic and hadronic showers in CC1, CC2, and S4 and the additional analysis of the hit strips of the AC detectors located along the trajectory of the initial particle, a rejection of ~10^5 was obtained.

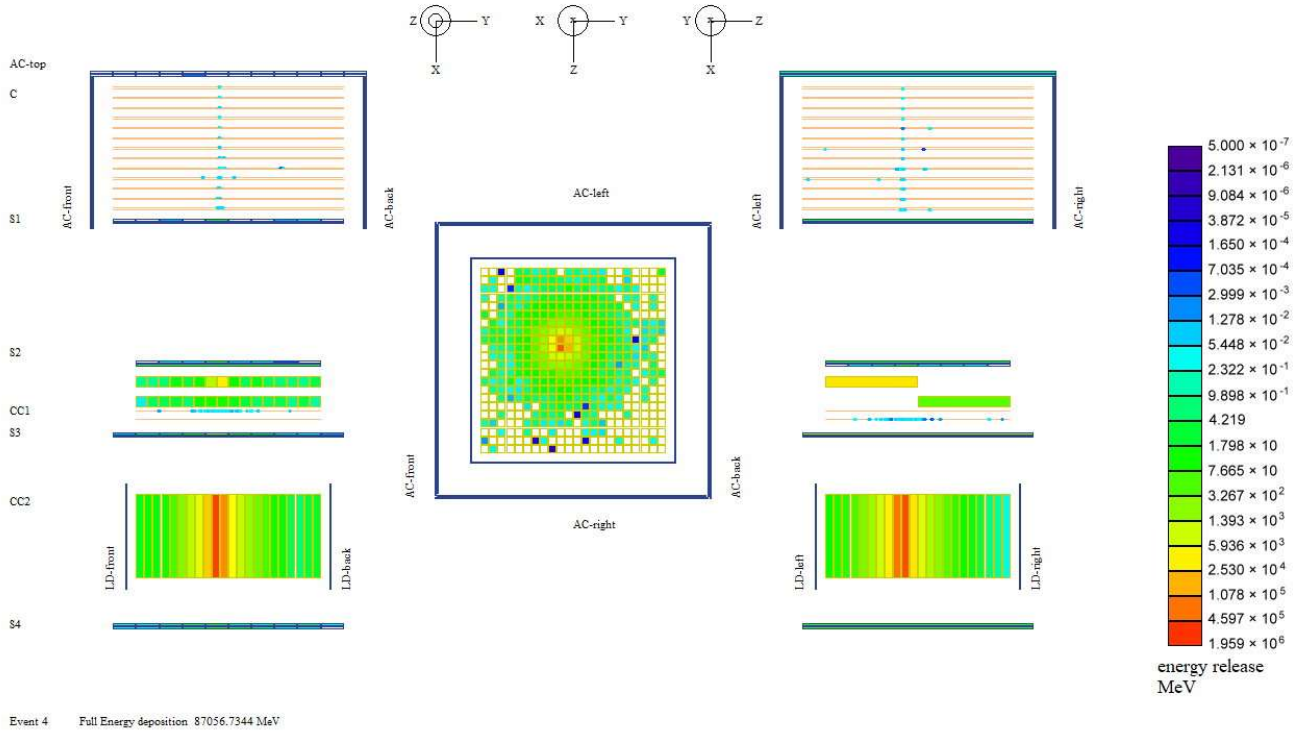

Figure 2. An example of an energy release simulation in the gamma-ray telescope's detectors. (the color scale of the energy release in MeV is shown in the right column).

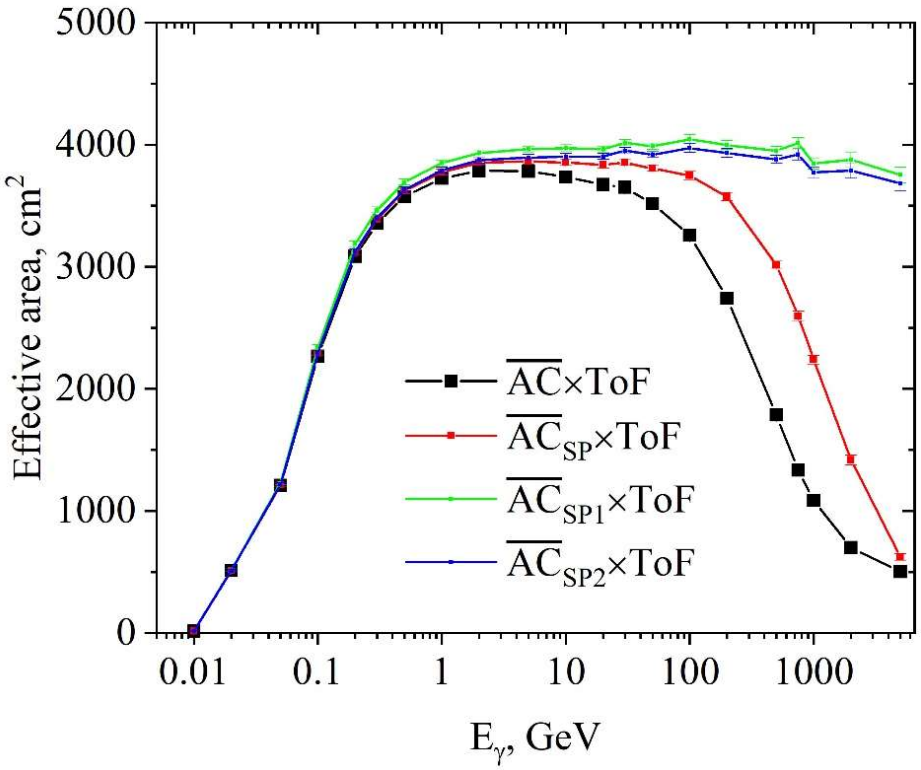

Figure 3. Dependence of the GAMMA-400 telescope's on-axis effective area on energy, using the triggers $\overline{AC} \times$ ToF (black), $\overline{AC_{SP}} \times$ ToF (red), $\overline{AC_{SP1}} \times$ ToF (green), and $\overline{AC_{SP2}} \times$ ToF (blue).

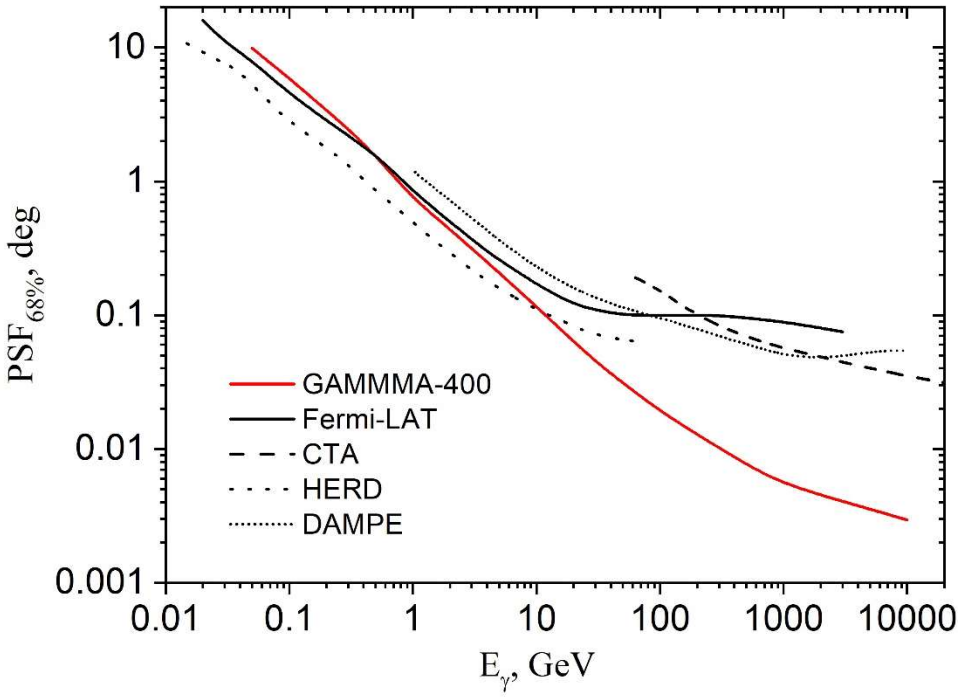

Figure 4. Dependence of the GAMMA-400 telescope's angular resolution on energy, in comparison with Fermi-LAT, CTA, HERD, and DAMPE.

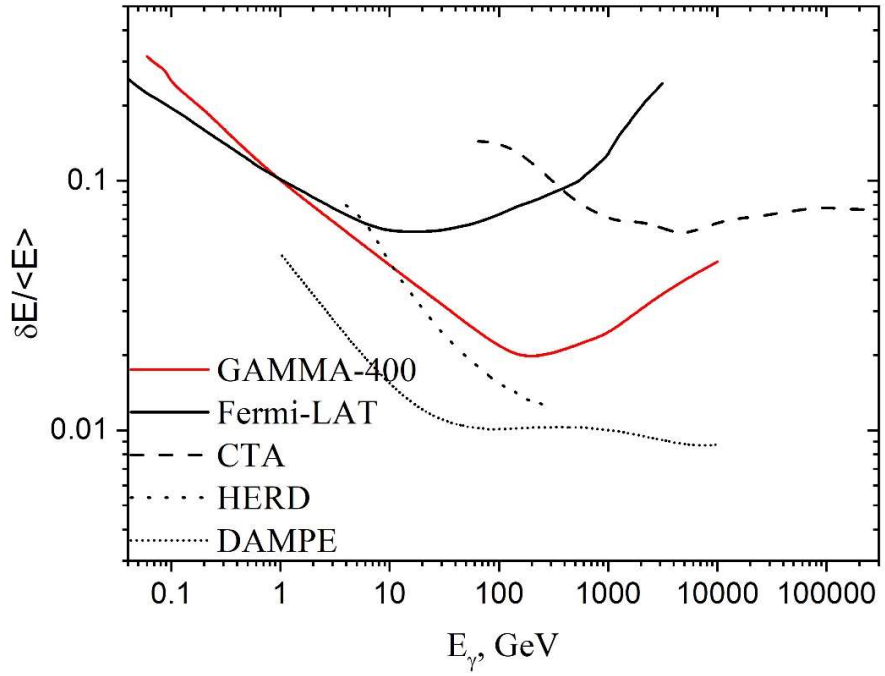

Figure 5. Dependence of the GAMMA-400 telescope's on-axis energy resolution on energy, in comparison with Fermi-LAT, CTA, HERD, and DAMPE.

2.2. Gamma-Ray Bursts

The GAMMA-400 telescope can also record GRBs from the top-down and lateral directions. When recording GRBs using the lateral aperture, the GAMMA-400 telescope's total effective field of view is ~6 sr. The GAMMA-400 telescope will allow us to detect ~15 GRBs per year.

2.3. Electron + Positron Detection

The GAMMA-400 telescope will also measure CR electron + positron fluxes from the top-down and lateral directions around the calorimeter. For these directions, the energy resolutions are ~2% and <1%, respectively. Figure 6 shows an example of a simulation of the energy release in the GAMMA-400 detectors for a 1-TeV electron coming from the left lateral direction. It is shown that for an electron from the left lateral direction, a significant amount of of backsplash hits the AC, converter, S1, S2, S3, and S4, and produces a deep shower in CC2; only the track continues in CC2.

Table 1 shows a performance comparison for the GAMMA-400 (top-down and lateral aperture) and Fermi-LAT [24] telescopes. It can be seen that due to the large area of the calorimeter (0.7 m^2 for the top-down and 1.0 m^2 for the lateral aperture) and the thickness of the calorimeter (18 X_0 for the top-down and 43 X_0 for the lateral aperture), the GAMMA-400 telescope can improve the electron + positron data statistics.

Table 1. Comparison of performance when detecting electrons + positrons for the GAMMA-400 (top-down and lateral aperture) and Fermi-LAT telescopes.

	GAMMA-400		**Fermi-LAT**
Aperture	**Top–Down**	**Four Lateral Sides**	**Top–Down**
Acceptance, m^2 sr	~0.3 (E_e = 100 GeV)	~0.5 (E_e = 100 GeV)	2.5
Proton rejection factor	~10^4	~10^4	~10^4
Calorimeter area, m^2	0.7	4 × 0.24	0.85
Calorimeter thickness, X_0	18	43	8.6

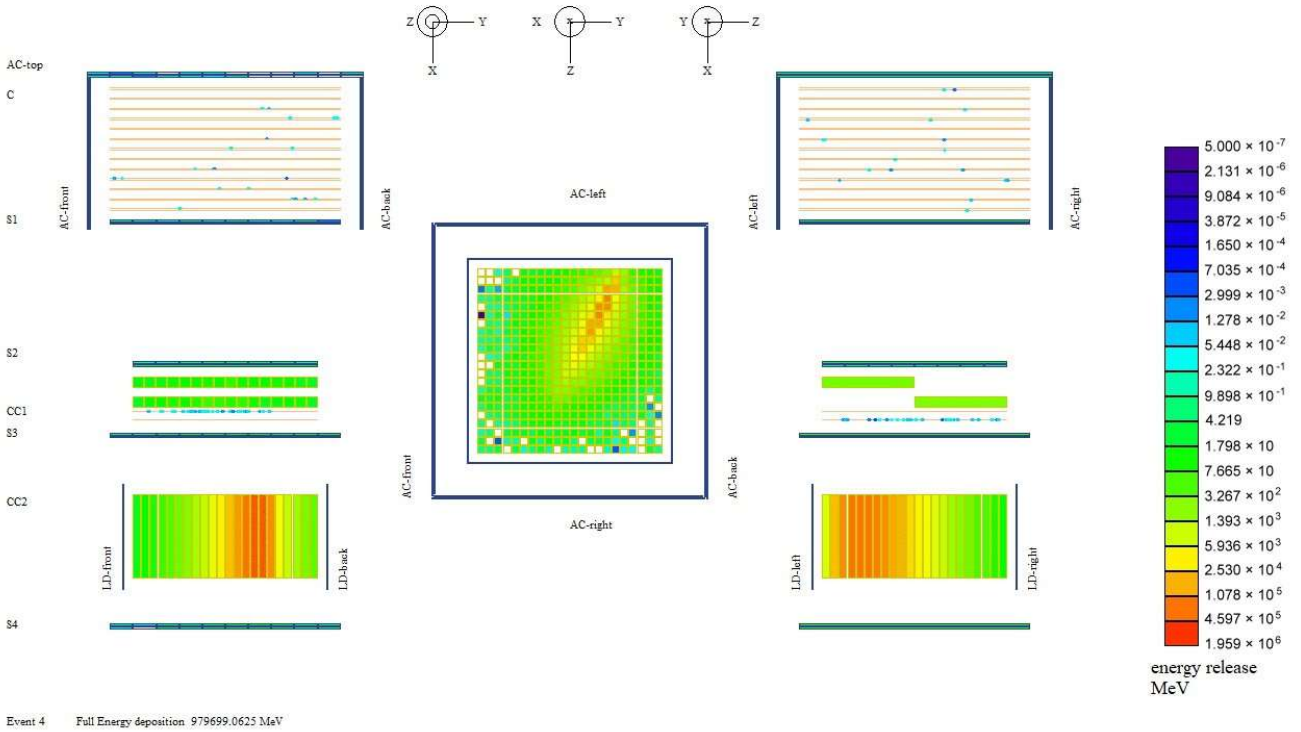

Figure 6. The example of an energy release simulation in the GAMMA-400 detectors (the color scale of the energy release is shown in MeV in the right column).

2.4. The Preliminary GAMMA-400 Scientific Program

The GAMMA-400 gamma-ray telescope has the following several advantages in comparison with current and future space-based and ground-based instruments:

(1) The GAMMA-400 gamma-ray telescope will continuously operate in a high orbit with a radius of ~200,000 km (after 6 months from its launch) in point-source mode with 100% efficiency over a long period of time (~100 days), with an aperture of ±45° in contrast to the scanning mode of other instruments;

(2) The GAMMA-400 gamma-ray telescope has a high angular resolution of ~0.01° (E_γ = 100 GeV) due to the high coordinate resolution in the SciFi coordinate detectors in the C and CC1 and the long arm between the coordinate detectors in the C and CC1;

(3) The GAMMA-400 gamma-ray telescope has a high energy resolution of ~2% (E_γ = 100 GeV) and the ability to detect incident particles from the top-down and lateral directions;

(4) The GAMMA-400 gamma-ray telescope is very good at separating gamma rays from the background of cosmic rays and backscattering events, as well as for the electrons + positrons from protons.

2.5. The GAMMA-400 Experiment Addresses Important Scientific Problems Remaining Relevant to Date

(1) The high-energy resolution provides the possibility of searching for features in the energy spectra of high-energy gamma-ray emissions up to energies of 1000 GeV, which can be associated with the annihilation or decay of dark matter particles (the most popular DM candidates are WIMPs and ALPs);

(2) The high angular resolution provides the possibility of studying discrete gamma-ray sources and identifying them (according to the fourth Fermi-LAT catalog, gamma-ray emissions from ~6500 sources were recorded, and ~30% of them were not identified);

(3) The high angular resolution also provides the possibility of studying the extended discrete sources' spatial structures in detail;
(4) The high angular resolution makes it possible to significantly reduce the influence of the background within the potential detection of gamma rays from pair halos around AGNs;
(5) The highly accurate event timing of several μs (due to the AC and ToF time resolutions of ~200 ps and the instrument timing interface accuracy of several μs) provides the possibility to study the source variability, including recording gamma-ray emissions from millisecond pulsars, and to explain the excess of gamma-ray emissions from the Galactic center;
(6) Searching for and studying GRBs will be carried out when a gamma-ray emission is detected from both top-down along the axis of the gamma-ray telescope and from four lateral directions;
(7) Simultaneous observations of discrete gamma-ray sources will be carried out jointly with X-ray telescopes, ground-based facilities, and optical, radio, and neutrino telescopes. Even if the GAMMA-400 telescope is anticipated to have a slightly lower degree of sensitivity to point sources in comparison with the Fermi-LAT telescope, it will be able to detect nearby extragalactic sources, including AGNs, in a wider energy range, beginning from about 20 MeV. Moreover, simultaneous observations with ART-XC could be more valuable given that both detectors will be co-directional;
(8) CR electron + positron fluxes will be recorded from top-down directions along the axis of the gamma-ray telescope at energies of up to several TeV (with a calorimeter thickness of 18 X_0) and from four lateral directions at energies of up to ~20 TeV (with a calorimeter thickness of 43 X_0) and will obtain significantly better measurement statistics.

The observations made using the Fermi-LAT gamma ray telescope have revealed many new types of flare sources: the so-called transients. Among them are quasi-periodic sources and sources that flare up only once. The study of their nature is declared one of the main goals of MeV-range telescopes and ground-based TeV-range gamma-ray telescopes. The absence of an instrument operating in the range of ~0.1–1000 GeV significantly impairs their capabilities.

The GAMMA-400 experiment will help solve the main problems that currently exist when measuring the spectrum of cosmic-ray electrons and positrons at high energies (100 GeV and above). The main advantages of the GAMMA-400 experiment are associated, firstly, with the good basic parameters of the instrument—its energy resolution and geometric factors—and secondly with the high reliability of the methodological measurement results. In fact, this is related to the implementation of two independent methods of electron recording (recording from the top-down direction, along the telescope axis, and recording from lateral directions) in one telescope.

3. Astrophysical Observatory

The new GAMMA-400 astrophysical observatory is being developed in Russia. It will consist of the Navigator spacecraft platform (being developed by the Lavochkin Association, https://www.laspace.ru/ru/activities/projects/gamma-400/, accessed on 2 August 2023), the GAMMA-400 gamma-ray telescope (being developed mainly by the Lebedev Physical Institute (https://gamma400.lebedev.ru/indexeng.html, accessed on 2 August 2023), and the National Research Nuclear University "MEPhI") and additional instruments (the ART-XC X-ray telescope with an energy range of 5–30 keV and magnetic plasma detectors that are being developed by the Space Research Institute of the Russian Academy of Sciences).

The Navigator spacecraft platform will have a possibility of pointing to any astrophysical source with an accuracy of 30″. The scientific payload will have the following characteristics: a mass of ~3000 kg, a power consumption of 2000 W, and a telemetry downlink of 100 GB/day.

The GAMMA-400 astrophysical observatory will be initially launched into a highly elliptical orbit with the following preliminary parameters: an apogee of 300,000 km, a perigee of 500 km, an inclination of 51.4°, a 7-day orbital period, and a lifetime of more than 7 years. After ~6 months, the orbit will be transformed into an approximately circular orbit with a radius of ~200,000 km due to the influence of the gravitational disturbances of the Sun, Moon, and Earth. Therefore, the observatory will not suffer from the Earth's occultation and will be outside the radiation belts. This is a great advantage in comparison with low-Earth orbit. The GAMMA-400 gamma-ray telescope will run continuously in a point-source operating mode for a long time, ~100 days, in contrast to the scanning modes for the current Fermi-LAT and future HERD [25] and AMS-100 [26] experiments. The launch of the GAMMA-400 space observatory is scheduled for ~2030.

4. Conclusions

The upcoming GAMMA-400 experiment will be implemented aboard the Russian astrophysical space observatory, which will be operating in a highly elliptical orbit for a period of 7 years to provide new data on gamma-ray emissions and cosmic-ray electron + positron fluxes that mainly originate from the galactic plane, the Galactic Center, and the Sun. A continuous point-source mode with an experimental duration of up to ~100 days will be the main operating mode. The GAMMA-400 gamma ray telescope will study high-energy emissions of gamma rays of up to several TeV and cosmic-ray electrons + positrons of up to ~20 TeV. The GAMMA-400 gamma-ray telescope will have a never—before-seen angular resolution, high energy and time resolutions, and a very good separation efficiency for separating gamma rays from the cosmic-ray background and the electrons + positrons from protons. A distinctive feature of the GAMMA-400 gamma-ray telescope is its wonderful angular resolution for energies of >30 GeV (0.01° for E_γ = 100 GeV), which exceeds the resolutions of current space-based and ground-based gamma ray telescopes by a factor of 5–10. The GAMMA-400 studies can reveal gamma-ray emissions from the annihilation or decay of dark matter particles, identify many unassociated discrete sources, explore the extended sources' structures, and improve the data on cosmic-ray electron + positron spectra for energies of >30 GeV. The Gamma-400 space observatory launch is scheduled for ~2030.

Author Contributions: Investigation, S.I.S., I.V.A., A.I.A., A.G.M., M.V.R. and N.Y.P.; formal analysis, A.V.B., V.V.M. and Y.T.Y.; software, I.V.C. and M.D.K.; conceptualization, A.M.G.; project administration, O.D.D.; methodology, A.E.E. and P.Y.M.; data curation, M.G.K. and A.A.L.; writing—review and editing, S.A.L.; supervision writing—original draft, N.P.T. All authors have read and agreed to the published version of the manuscript.

Funding: This study was supported by the Russian State Space Corporation ROSCOSMOS, in part by the Ministry of Science and Higher Education of the Russian Federation under the Project "Fundamental and applied research of cosmic rays" (contract no. FSWU–2023-0068).

Data Availability Statement: http://gamma400.lebedev.ru/index.html accessed on 2 August 2023.

Conflicts of Interest: The authors declare no conflict of interest.

References

1. Abdollahi, S.; Acero, F.; Baldini, L.; Ballet, J.; Bastieri, D.; Bellazzini, R.; Berenji, B.; Berretta, A.; Bissaldi, E.; Blandford, R.D.; et al. Incremental Fermi large area telescope fourth source catalog. *Astrophys. J. Suppl. Ser.* **2022**, *260*, 53. [CrossRef]
2. Abdollahi, S.; Acero, F.; Ackermann, M.; Ajello, M.; Atwood, W.B.; Axelsson, M.; Baldini, L.; Ballet, J.; Barbiellini, G.; Bastieri, D.; et al. Fermi large area telescope fourth source catalog. *Astrophys. J. Suppl. Ser.* **2020**, *247*, 33. [CrossRef]
3. Xing, Y.; Wang, Z.; Zheng, D.; Li, J. On the Gamma-Ray Emission of the Andromeda Galaxy M31. *Astrophys. J. Lett.* **2023**, *945*, L22. [CrossRef]
4. Belotsky, K.; Shlepkina, E.; Soloviev, M. Theoretical indication of a possible asymmetry in gamma-radiation between Andromeda halo hemispheres due to Compton scattering on electrons from their hypothetical sources in the halo. *arXiv* **2020**, arXiv:2011.04689.
5. Dermer, C.; Giebels, B. Active galactic nuclei at gamma-ray energiesNoyaux actifs de galaxie dans le domaine des rayons gamma. *C. R. Phys.* **2016**, *17*, 594–616. [CrossRef]

6. Ajello, M.; Arimoto, M.; Axelsson, M.; Baldini, L.; Barbiellini, G.; Bastieri, D.; Bellazzini, R.; Bhat, P.N.; Bissaldi, E.; Blandford, R.D.; et al. A decade of gamma-ray bursts observed by Fermi-LAT: The second GRB catalog. *Astrophys. J.* **2019**, *878*, 52. [CrossRef]
7. Von Kienlin, A.; Meegan, C.A.; Paciesas, W.S.; Bhat, P.N.; Bissaldi, E.; Briggs, M.S.; Burns, E.; Cleveland, W.H.; Gibby, M.H.; Giles, M.M.; et al. The Fourth Fermi-GBM Gamma-Ray Burst Catalog: A Decade of Data. *Astrophys. J.* **2020**, *893*, 46. [CrossRef]
8. Lien, A.; Sakamoto, T.; Barthelmy, S.D.; Baumgartner, W.; Chen, K.; Collins, N.R.; Cummings, J.; Gehrels, N.; Krimm, H.A.; Markwardt, C.B.; et al. The Third SWIFT Burst Alert Telescope Gamma-Ray Burst Catalog. *Astrophys. J.* **2016**, *829*, 7. [CrossRef]
9. Leane, R.K.; Slatyer, T.R.; Beacom, J.F.; Ng, K.C. GeV-scale thermal WIMPs: Not even slightly ruled out. *Phys. Rev. D* **2018**, *98*, 023016. [CrossRef]
10. Calore, F.; Carenza, P.; Giannotti, M.; Jaeckel, J.; Mirizzi, A. Bounds on axionlike particles from the diffuse supernova flux. *Phys. Rev. D* **2020**, *102*, 123005. [CrossRef]
11. Chang, J.; Adams, J.H.; Ahn, H.S.; Bashindzhagyan, G.L.; Christl, M.; Ganel, O.; Guzik, T.G.; Isbert, J.; Kim, K.C.; Kuznetsov, E.N.; et al. An excess of cosmic ray electrons at energies of 300–800 GeV. *Nature* **2008**, *456*, 362–365. [CrossRef]
12. Abdollahi, S.; Ackermann, M.; Ajello, M.; Atwood, W.B.; Baldini, L.; Barbiellini, G.; Bastieri, D.; Bellazzini, R.; Bloom, E.D.; Bonino, R.; et al. Cosmic-ray electron-positron spectrum from 7 GeV to 2 TeV with the Fermi Large Area Telescope. *Phys. Rev. D* **2017**, *95*, 082007. [CrossRef]
13. Adriani, O. et al. [Pamela Collaboration]); Adriani, O.; Barbarino, G.C.; Bazilevskaya, G.A.; Bellotti, R.; Boezio, M.; Bogomolov, E.V.; Bongi, M.; Bonvicini, V.; Bottai, S.; et al. Ten years of PAMELA in space. *Nuevo C* **2017**, *10*, 473–522.
14. Aguilar, M.; Aisa, D.; Alpat, B.; Alvino, A.; Ambrosi, G.; Andeen, K.; Arruda, L.; Attig, N.; Azzarello, P.; Bachlechner, A.; et al. Precision Measurement of the (e^+ + e^-) Flux in Primary Cosmic Rays from 0.5 GeV to 1 TeV with the Alpha Magnetic Spectrometer on the International Space Station. *Phys. Rev. Lett.* **2014**, *113*, 221102. [CrossRef]
15. Adriani, O.; Akaike, Y.; Asano, K.; Asaoka, Y.; Bagliesi, M.G.; Berti, E.; Bigongiari, G.; Binns, W.R.; Bonechi, S.; Bongi, M.; et al. Extended measurement of the cosmic-ray electron and positron spectrum from 11 GeV to 4.8 TeV with the calorimetric electron telescope on the International Space Station. *Phys. Rev. Lett.* **2018**, *120*, 261102. [CrossRef] [PubMed]
16. Ambrosi, G. et al. [DAMPE Collaboration] Direct detection of a break in the teraelectronvolt cosmic-ray spectrum of electrons and positrons. *Nature* **2017**, *552*, 63–66. [CrossRef]
17. Tridon, D.B.; Colin, P.; Cossio, L.; Doro, M.; Scalzotto, V. Measurement of the cosmic electron plus positron spectrum with the MAGIC telescopes. *arXiv* **2011**, arXiv:1110.4008.
18. Staszak, D. et al. [for the VERITAS Collaboration] A Cosmic-ray Electron Spectrum with VERITAS. *arXiv* **2015**, arXiv:1508.06597.
19. Aharonian, F.; Akhperjanian, A.G.; Anton, G.; de Almeida, U.B.; Bazer-Bachi, A.R.; Becherini, Y.; Behera, B.; Bernlöhr, K.; Bochow, A.; Boisson, C.; et al. Probing the ATIC peak in the cosmic-ray electron spectrum with H.E.S.S. *Astron. Astrophys.* **2009**, *508*, 561–564. [CrossRef]
20. Dogiel, V.; Fradkin, M.; Kurnosova, L.; Razorenov, L.; Rusakovich, M.; Topchiev, N. Some tasks of observational gamma-ray astronomy in the energy range 5-400 GeV. *Space Sci. Rev.* **1988**, *49*, 215–226. [CrossRef]
21. Ginzburg, V.L.; Kaplin, V.A.; Karakash, A.I.; Kurnosova, L.V.; Labenskii, A.G.; Runtso, M.F.; Soldatov, A.P.; Topchiev, N.P.; Fradkin, M.I.; Chernichenko, S.K.; et al. Development of the GAMMA-400 gamma-ray telescope to record cosmic gamma rays with energies up to 1 TeV. *Cos. Res.* **2007**, *45*, 449–451. [CrossRef]
22. Suchkov, S.I.; Arkhangelskiy, A.I.; Baskov, V.A.; Galper, A.M.; Dalkarov, O.D.; L'vov, A.I.; Pappe, N.Y.; Polyansky, V.V.; Topchiev, N.P.; Chernysheva, I.V. Calibrating the prototype calorimeter for the GAMMA-400 gamma-ray telescope on the positron beam at the Pakhra accelerator. *Instrum. Exp. Tech.* **2021**, *64*, 669–675. [CrossRef]
23. Topchiev, N.; Galper, A.; Arkhangelskaja, I.; Arkhangelskiy, A.; Bakaldin, A.; Cherniy, R.; Chernysheva, I.; Gudkova, E.; Gusakov, Y.; Dalkarov, O.; et al. Gamma- and Cosmic-Ray Observations with the GAMMA-400 Gamma-Ray Telescope. *Adv. Space Res.* **2022**, *70*, 2773–2793. [CrossRef]
24. Atwood, W.B.; Abdo, A.A.; Ackermann, M.; Althouse, W.; Anderson, B.; Axelsson, M.; Baldini, L.; Ballet, J.; Band, D.L.; Barbiellini, G.; et al. The large area telescope on the Fermi gamma-ray telescope mission. *Astrophys. J.* **2009**, *697*, 1071–1102. [CrossRef]
25. Cattaneo, P.W. et al. [on behalf of the HERD Collaboration] The space station based detector HERD: Precise high energy cosmic rays physics and multimessenger astronomy. *Nucl. Part. Phys. Proc.* **2019**, *306–308*, 85–91.
26. Schael, S.; Atanasyan, A.; Berdugo, J.; Bretz, T.; Czupalla, M.; Dachwald, B.; von Doetinchem, P.; Duranti, M.; Gast, H.; Karpinski, W.; et al. AMS-100: The next generation magnetic spectrometer in space—An international science platform for physics and astrophysics at Lagrange point 2. *Nucl. Instrum. Methods Phys. Res. Sect. A* **2019**, *944*, 162561.